Appendix A: Key definitions

Crop Land Productivity (Crop Yield)

Land productivity*, or crop yield, is a measurement of the amount of crop that is harvested per unit of land area. It is often used for cereal, grain or legume and is normally measured in metric tons per hectare (or kilograms per hectare)* (Investopedia, 2015)*.* In China, the crop yields of cereals have increased from 4,75 to 5,89 tonnes per hectare from 2000 to 2013. This value is higher than the world average of 3,82, but here are countries (like Belgium, the Netherlands and Germany) that reach average yields of 7-10 tonnes per hectare, so it is possible that crop yields per hectare of China will keep increasing in the future (The World Bank, 2015a).

Crop Water Productivity

Crop water productivity (CWP) (also known as water use efficiency (WUE)) is an efficiency term expressing the amount of marketable product (usually kg of crop) divided by the amount of water (usually in cubic meters) needed to produce that amount of product. The water used is defined as the crop evapotranspiration. This is a combination of evaporation from soil surface and plant transpiration. Representative values of CWP for cereals at field level can vary between 0,10 and 4 kg/m^3 (Kijne, Barker and Molden, 2003)

When considering this relation from a physical point of view, one should consider transpiration only. The partitioning of evapotranspiration in evaporation and transpiration in field experiments is, however, difficult and therefore not a practical solution. Moreover, evaporation is always a component related to crop specific growth, tillage and water management practices, and this water is no longer available for other usage or reuse in the basin. Since evapotranspiration is based on root water uptake, supplies from rainfall, irrigation and capillary rise are integrated.

The great challenge of the agricultural sector is to produce more food from less water, which can be achieved by increasing Crop Water Productivity (CWP). Based on a review of 84 literature sources with results of experiments not older than 25 years, it was found that the ranges of CWP of wheat, rice, cotton and maize exceed in all cases those reported by FAO earlier. Globally measured average CWP values per unit water depletion are 1.09, 0.23 and 1.80 kg m−3 for wheat, rice, and maize, respectively. The range of CWP is very large (wheat, 0.6–1.7 kg m−3; rice, 0.6–1.6 kg m−3; 0.14–0.33 kg m−3 and maize, 1.1–2.7 kg m−3) and thus offers tremendous opportunities for maintaining or increasing agricultural production with 20–40% less water resources. The variability of CWP can be ascribed to: (i) climate; (ii) irrigation water management and (iii) soil (nutrient) management, among others. The vapour pressure deficit is inversely related to CWP. Vapour pressure deficit decreases with latitude, and thus favourable areas for water wise irrigated agriculture are located at the higher latitudes. The most outstanding conclusion is that CWP can be increased significantly if irrigation is reduced and crop water deficit is intendently induced (Zwart and Bastiaanssen, 2004).

Water Footprint of crops

The concept of the water footprint was introduced by Hoekstra (2003b). The water footprint of a product is expressed in water volume per unit of product (usually m^3 ton^{-1}) and is the sum of the water footprints of the process steps taken to produce the product.

There are three classes of water footprint: Green, blue and grey. They have the following definitions:

Green water footprint *– Volume of rainwater consumed during the production process. This is particularly relevant for agricultural and forestry products (products based on crops or wood),* *where it refers to the total rainwater evapotranspiration (from fields and plantations) plus the water incorporated into the harvested crop or wood.*

Blue water footprint – *Volume of surface and groundwater consumed as a result of the production of a good or service. Consumption refers to the volume of freshwater used and then evaporated or incorporated into a product. It also includes water abstracted from surface or groundwater in a catchment and returned to another catchment or the sea. It is the amount of water abstracted from groundwater or surface water that does not return to the catchment from which it was withdrawn.*

Grey water footprint – *The grey water footprint of a product is an indicator of freshwater pollution that can be associated with the production of a product over its full supply chain. It is defined as the volume of freshwater that is required to assimilate the load of pollutants based on natural background concentrations and existing ambient water quality standards. It is calculated as the volume of water that is required to dilute pollutants to such an extent that the quality of the water remains above agreed water quality standards.*

(Water Footprint Network, 2015)

Appendix B: (Emission) Scenarios

Scenarios are used to analyse situations with uncertain outcomes. The goal of these scenarios is not to predict the future, but to better understand uncertainties and alternative futures, in order to consider how robust different decisions or options may be under a wide range of possible futures. In climate change research, scenarios describe plausible trajectories of different aspects of the future that are constructed to investigate the potential consequences of anthropogenic climate change (IPCC, 2014c).

In 2007, the IPCC requested the scientific community to develop a new set of scenarios, because the existing SRES (Special Report on Emissions Scenarios) scenarios needed to be updated (van Vuuren et al., 2011b). The process by which these new scenarios are created differs from earlier scenario development. In the past, the socio-economic scenarios were produced first, which lead to alternative future greenhouse gas and aerosol emissions. After that the implications of these emissions and the different socio-economic futures on natural and human systems were assessed. This linear process takes approximately 10 years (IPCC, 2014d). The new process is not linear but parallel, in order to shorten the time required for development and application. It contains three main phases:

1. Initial phase, developing a set of pathways for emissions, concentrations an radiative forcing
2. Parallel phase, made up of both the development of new socio-economic storylines and climate model projections
3. Integration phase, combining the first two phases.

The pathways created in phase one are called 'Representative Concentration Pathways (RCPs). By design, these RCPs as a set cover the range of radiative forcing levels examined in the open literature (van Vuuren et al., 2011b). There are four RCPs, ranging in radiative forcing from 2.6 to 8.5 W/m^2, with two pathways in between with a forcing of 4.5 and 6 W/m^2 (Figure B1).

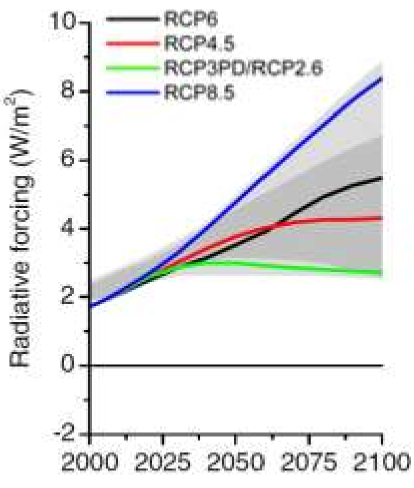

Figure B1; Radiative Forcing of the Representative Concentration Pathways. From van Vuuren et al (2011) The Representative Concentration Pathways: An Overview. Climatic Change, 109 (1-2), 5-31. . The light grey area captures 98% of the range in previous IAM scenarios, and dark grey represents 90% of the range.

Note that RCPs in themselves are not linked to any one socio-economic scenario: each RCP is consistent with many socio-economic scenarios because different socio-economic futures could give rise to similar changes in atmospheric composition (IPCC, 2014d). Most RCP scenarios can however be linked SRES scenarios that have a similar increase in temperature by 2100, as can be seen in Table B1 and Table B2. This can be used to compare studies using RCPs to studies using SRES scenarios.

Table B1; The different RCP scenarios, their radiative forcing, CO_2 equivalent, increase in temperature by 2100, a description of the pathway to the future climate and the SRES scenarios that have similar temperature increases by 2100 (Rogelj, Meinshausenn and Knutti, 2012).

Name	Radiative forcing	CO_2 equiv (p.p.m.)	Temp anomaly (°C)	Pathway	SRES temp anomaly equiv
RCP8.5	8.5 Wm² in 2100	1370	4.9	Rising	SRES A1F1
RCP6.0	6 Wm² post 2100	850	3.0	Stabilization without overshoot	SRES B2
RCP4.5	4.5 Wm² post 2100	650	2.4	Stabilization without overshoot	SRES B1
RCP2.6 (RCP3PD)	3Wm² before 2100, declining to 2.6 Wm² by 2100	490	1.5	Peak and decline	None

Table B2; The RCP scenarios, the SRES scenarios with a similar temperature increase by 2100 and the differences between the RCP and SRES scenarios (Rogelj, Meinshausenn and Knutti, 2012).

Main similarities and differences between temperature projections for SRES scenarios and RCPs.		
RCP	**SRES scenario with similar median temp increase by 2100**	**Particular differences**
RCP3PD	None	The ratio between temperature increase and net radiative forcing in 2100 is 0:88 C(Wm^{-2})$^{-1}$ for RCP3-PD, whereas all other scenarios show a ratio of about 0:62 C(Wm^{-2})$^{-1}$; that is, RCP3-PD is closer to equilibrium in 2100 than the other scenarios.
RCP4.5	SRES B1	Median temperatures in RCP4.5 rise faster than in SRES B1 until mid-century, and slower afterwards.
RCP6	SRES B2	Median temperatures in RCP6 rise faster than in SRES B2 during the three decades between 2060 and 2090, and slower during other periods of the twenty-first century.
RCP8.5	SRES A1FI	Median temperatures in RCP8.5 rise slower than in SRES A1FI during the period between 2035 and 2080, and faster during other periods of the twenty-first century.

Appendix C: Climate Models

To order to "predict" the future climate responses to increasing levels of greenhouse gas, numerical models are used. The most advanced models are called Global Climate Models, or General Circulation Models (GCMs). They represent the physical processes in the atmosphere, ocean, cryosphere (areas that are covered in ice) and land surface (IPCC, 2013) using a system of differential equations based on the basic laws of physics, fluid motion, and chemistry.

In GCMs the climate is represented using a three dimensional grid over the globe (Figure C1). The resolution usually is between 250 and 600 km horizontally and the grid contains between 10 and 30 vertical layers. This resolution is quite course for impact assessments like this study, so a downscaling procedure has to be used (IPCC, 2013).

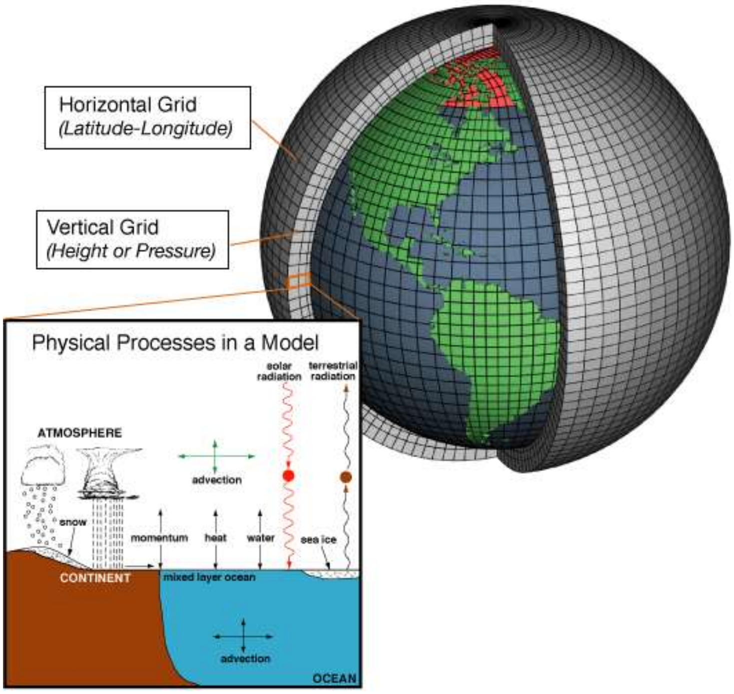

Figure C1; The grid and physical processes of a climate model (NOAA, 2007)

Another downside is that many physical processes, like those related to clouds, also have a smaller scale therefore cannot be properly modelled. This means their know properties must be averaged over the larger grid. This is called parameterization. This is a source of uncertainty in the GCM simulations of future climate. Other sources of uncertainty are related to the simulation of various feedback mechanisms in models like water vapour and warming, clouds and radiation, ocean circulation an ice and snow reflection. Due to these uncertainties, different GCMs can simulate quite different responses to the same RCP scenario (IPCC, 2013).

Downscaling

The IPCC 5th assessment report uses the Delta Method for downscaling. This method is explained in a report by Ramirez-Villegas & Jarvis (2010). The downscaling method is based on '*thin plate spline spatial interpolation of anomalies (deltas) of original GCM outputs. Anomalies are* *interpolated between GCM cell centroids and are then applied to a baseline climate given by a high resolution surface'.* The method makes the following gross assumptions (CCAFS, 2015b):

1. Changes in climates vary only over large distances (i.e. as large as GCM side cell size)

2. Relationships between variables in the baseline ("current climates") are likely to be maintained towards the future

We acknowledge that these assumptions might not hold true in highly heterogeneous landscapes, where topography could cause considerable variations in anomalies (i.e. the Andes); however, the assumption is useful for relatively homogeneous or very homogeneous areas such as the Sahara, the Amazon, and other global areas with homogeneous landscapes. The process consists of the following steps:

1. Gathering of baseline data (current climates corresponding to WorldClim)

2. Gathering of full GCM timeseries

3. Calculation of 30 year running averages for present day simulations (1961-1990) and 7 future periods

4. Calculation of anomalies as the ***absolute difference*** *between future values in each of the 3 variables to be interpolated (minimum and maximum temperature, and total precipitation)*

5. Interpolation of these anomalies using centroids of GCM cells as points for interpolation

6. Addition of the interpolated surfaces to the current climates from WorldClim, using absolute sum for temperatures, and addition of relative changes for precipitation

7. Calculation of mean temperature as the average of maximum and minimum temperatures WorldClim and full GCM timeseries are freely available in the internet, whilst all other calculations are carried out by means of Geographic Information Systems (GIS) software. Used formats are NetCDF (for GCM outputs), ESRI-GRID (for WorldClim and final downscaled data), and ESRI-ASCII grids for providing standard and easy-of-use outputs to potential users of the data.

Available GCMs

The available models that use RCPs and are downscaled using the Delta Method are represented in Figure .

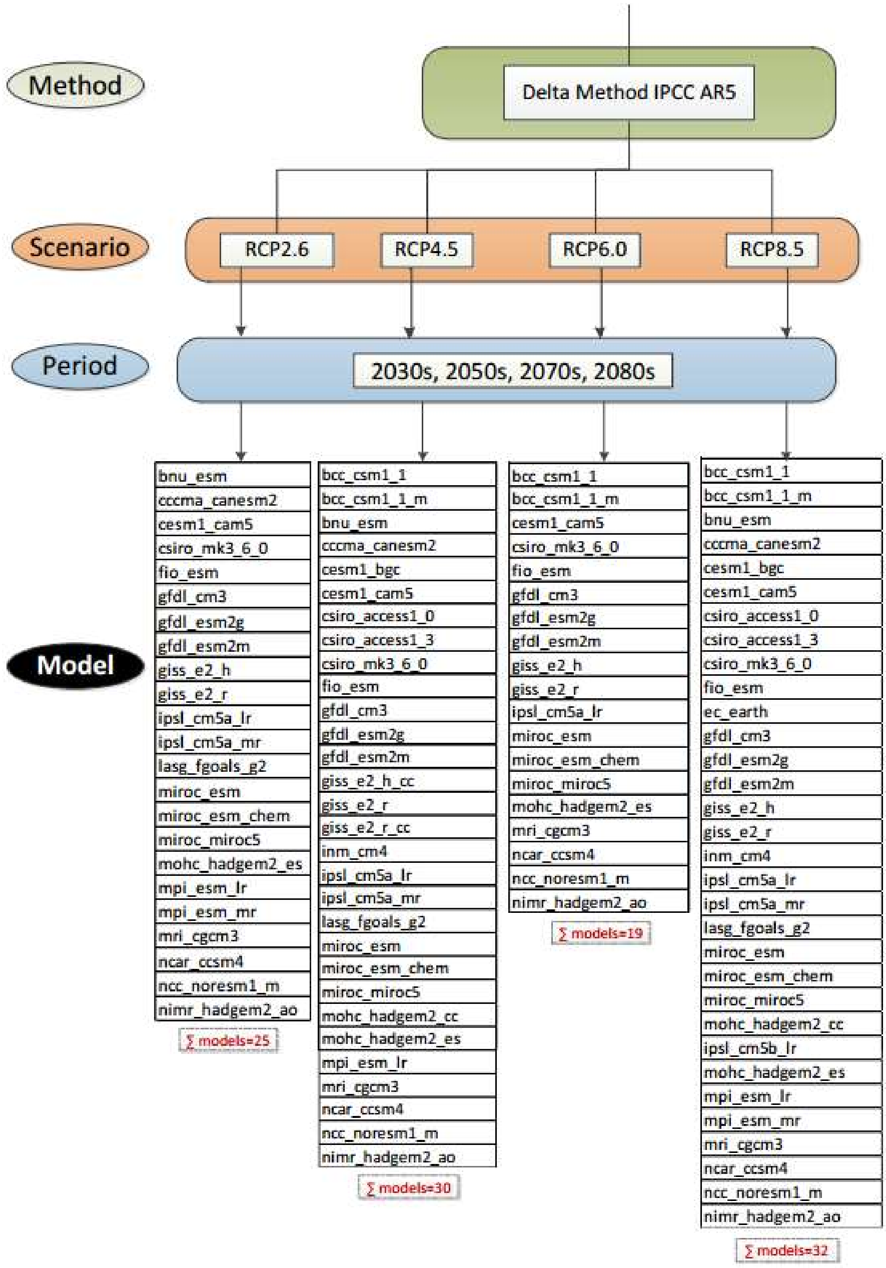

Figure C2; Representation of the GCMs available GCMs using RCPs and that are downscaled using the Delta Method (CCAFS, 2015a).

The models that are available for all four RCP scenarios are listed in table C1

Table C1; Climate models that are available for all four RCPs

#	Model Name	Developer / Name	Country	Resolution [km] (lon. x lat.) Atmosphere	Ocean	Reference
1	cesm1_cam5	Community Earth System Model – Community Athomosphere Model	United States	288 x 192	320 x 384	(Meehl et al., 2013)
2	csiro_mk3_6_0	Commonwealth Scientific Industrial Research Organisation (Australia)	Australia	192 x 96	192 x 189	(Rotstayn et al., 2010)
3	fio_esm	First Institute of Oceonography – Earth systems model	China	128 x 64	320 x 384	
4	gfdl_cm3	Geophysical Fluid Dynamics Laboratory – Climate model v3	United States			
5	gfdl_esm2g	Geophysical Fluid Dynamics Laboratory – Earth System Model	" "			
6	gfdl_esm2m	Geophysical Fluid Dynamics Laboratory – Earth system model	" "	144 x 90	360 x 200	(Dunne et al., 2012)
7	giss_e2_r	Goddart Institute of Space Studies (NASA)	United States	144 x 90	144 x 90	(Kim et al., 2012)
8	ipsl_cm5a_lr	Institut Pierre Simon Laplace	France	96 x 96	96 x 96	(Dufresne, Foujols and Denvil S., 2013)
9	miroc_esm	Model for Interdisciplinary Research on Climate – Earth System Model	Japan			
10	miroc_esm_chem	" "	" "			
11	miroc_miroc5	" "	" "	256 x 224	256 x 224	(Watanabe et al., 2010)
12	mohc_hadgem2_es	Hadley Centre Global Environment Model version 2 – Earth system	United Kingdom	192 x 145	320 x 216	(Martin et al., 2011)
13	mri_cgcm3	Meteorological Research Institute Coupled Global Climate Model	Japan?	320 x 160	360 x 368	(Yukimoto, 2011)
14	nimr_hadgem2_ao	Hadley Centre Global Environment model version 2 – Atmosphere Ocean	United Kingdom	192 x 144	230 x 216	(Johns et al., 2006)

GCM choice

Table C2. Ranking of GCMs based on temperature and precipiation

Model Name	T#	T# s	P # s	P # s	score	
csiro_mk3_6_0	5	0.6	**1**	0.1	3	Hot and Dry
ipsl_cm5a	3	0.3	3	0.4	4	
miroc_esm_chem	**1**	0.1	6	0.9	5	Hot and wet
mohc_hg2	3	0.3	5	0.7	5	
Mri_cgcm3	6	0.7	3	0.4	5	
fio_esm	9	1.0	1	0.1	6	Dry and Cold
miroc_esm	2	0.2	6	0.9	5	
giss_e2_r	8	0.9	2	0.3	6	
gfdl_cm3	2	0.2	7	1.0	6	
gfdl_esm2m	7	0.8	4	0.6	7	
Nimr_hadgem2	6	0.7	5	0.7	7	
cesm1_cam5	4	0.4	7	1.0	7	
gfdl_esm2g	9	1.0	4	0.6	8	
miroc_miroc5	5	0.6	**7**	1.0	8	Wet and Cold

Appendix D: AquaCrop

AquaCrop is a crop

water productivity model to simulate yield response to water developed by the Food and Agriculture Organisation of the United Nations (FAO) (Steduto and Raes , 2009) .

The model has the following components: The soil*, with its water balance*; the crop*, with its development, growth and yield processes; and* the atmosphere*, with its thermal regime, rainfall, evaporative demand and carbon dioxide concentration. Additionally, some* management *aspects are explicitly considered (e.g., irrigation, fertilization, etc.), as they will affect the soil water balance, crop development and therefore final yield. AquaCrop can also simulate crop growth under climate change scenarios (global warming and elevated carbon dioxide concentration)* (Raes et al., 2011)

There are several other crop models available in literature to simulate yield response to water, but these models are more complex and require an extended number of variables and input parameters not easily available for the diverse range of crops and sites around the world.

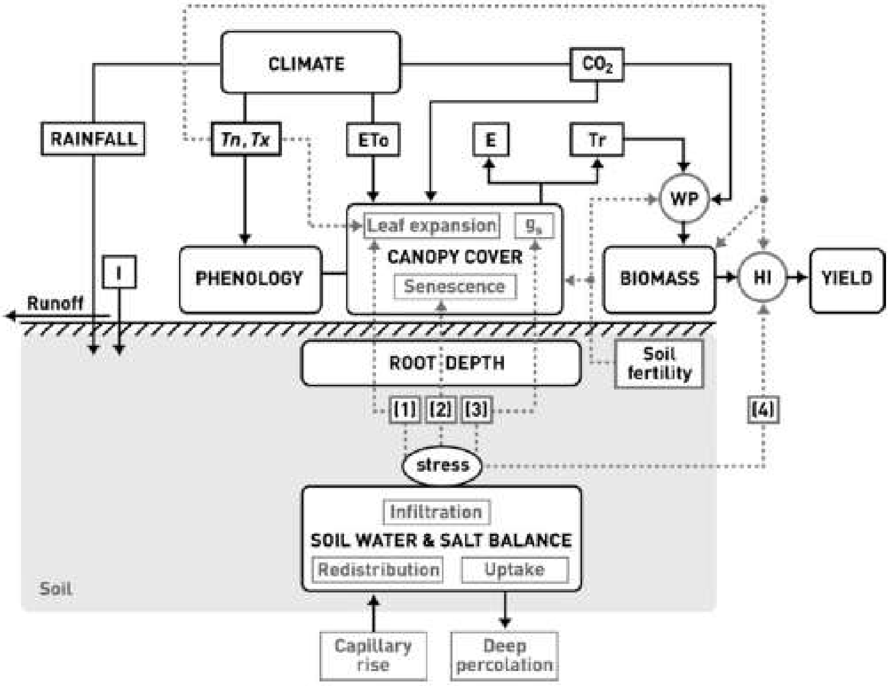

Figure 1.1b

Chart of *AquaCrop* indicating the main components of the soil–plant–atmosphere continuum and the parameters driving phenology, canopy cover, transpiration, biomass production, and final yield. [I, irrigation; T_n, minimum airtemperature; T_x, maximum air temperature; ET_0, reference evapotranspiration; E, soil evaporation; Tr, canopy transpiration; gs, stomatal conductance; WP, water productivity; HI, harvest index; CO_2, atmospheric carbon dioxide concentration; (1), (2), (3), (4), water stress response functions for leaf expansion, senescence, stomatal conductance and harvest index, respectively]. Continuous lines indicate direct links between variables and processes. Dashed lines indicate feedbacks. See section 1.2 for a more extensive description

The operation of AquaCrop consists the following processes:

1. Simulation of the soil water balance
2. Simulation of the green canopy development
3. Simulation of crop transpiration
4. Simulation of the above-ground biomass
5. Partitioning of biomass into yield

1. Soil water balance. The amount of water stored in the root zone is simulated by accounting for the incoming and outgoing water fluxes at its boundaries. The root zone depletion determines the magnitude of a set of water stress coefficients (Ks) affecting: (a) green canopy (CC) expansion, (b) stomatal conductance and hence transpiration (Tr) per unit CC, (c) canopy senescence and decline, (d) the harvest index (HI) and (e) the root system deepening rate;

2. Crop development. In the simulation of crop development, the canopy expansion is separated from the expansion of the root zone. The interdependence between shoot and root is indirect via water *stress. AquaCrop uses canopy cover to describe crop development. The canopy is a crucial feature of AquaCrop. Through its expansion, ageing, conductance and senescence, it determines the amount of water transpired (Tr), which in turns determines the amount of biomass produced (B) and the final yield (Y). If water stress occurs, the simulated CC will be less than the potential canopy cover (CCpot) for no stress conditions and the maximum rooting depth might not be reached (dark shaded areas in Fig. 1.2a);*

3. Crop transpiration (Tr). Crop transpiration is obtained by multiplying the evaporating power of the atmosphere (ETo) with a crop coefficient. The crop coefficient (Kcb) is proportional to CC and hence continuously adjusted. The evaporating power is expressed by the reference grass evapotranspiration (ETo) as determined by the FAO Penman-Monteith equation. If water stress induces stomatal closure, the water stress coefficient for stomatal conductance (Ks) reduces transpiration accordingly. Green canopy cover and duration represent the source for transpiration, stomatal conductance represents transpiration intensity;

4. Above ground biomass (B). The cumulative amount of water transpired (Tr) translates into a proportional amount of biomass produced through the biomass water productivity (Eq. 1.1c). In AquaCrop the water productivity normalized for atmospheric demand and air CO_2 concentrations (WP) is used. It expresses the strong relationship between photosynthetic CO_2 assimilation or biomass production and transpiration independently of the climatic conditions. Beyond the partitioning of biomass into yield (Step 5), there is no partitioning of above-ground biomass among various organs. This choice avoids dealing with the complexity and uncertainties associated with the partitioning processes, which remain among the least understood and most difficult to model;*

5. Partitioning of biomass into yield (Y). Given the simulated above ground biomass (B), crop yield is obtained with the help of the Harvest Index (Eq. 1.1c). In response to water and/or temperature stresses, HI is continuously adjusted during yield formation.

(Raes et al., 2011)

Appendix E. Precipitation Changes for Rainfed Maize under Scenario W85

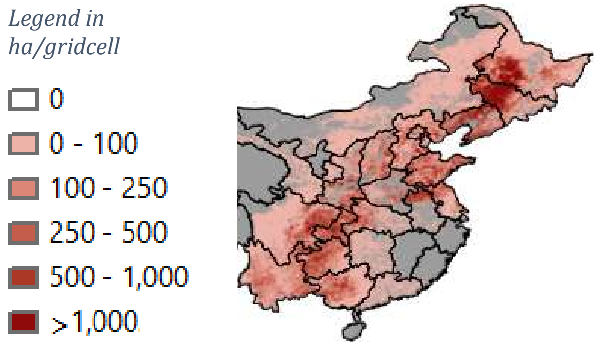

Figure E1. Planted area of rainfed maize.

Figure E1 shows the planted area of rainfed maize. In can clearly be seen that the highest planted areas form a line from the Southwest up to the Northeast.

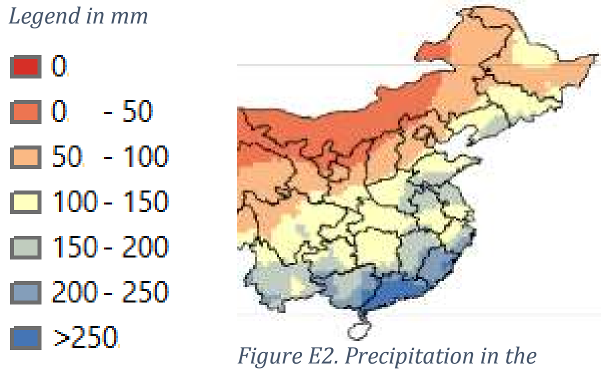

Figure E2. Precipitation in the growing period of maize in 2005.

Figure E2 shows the precipitation in the growing period of maize in 2005. In this year, most of the heavily planted area (darker red in Figure 1) is is in areas with 100 mm of precipitation a month or higher.

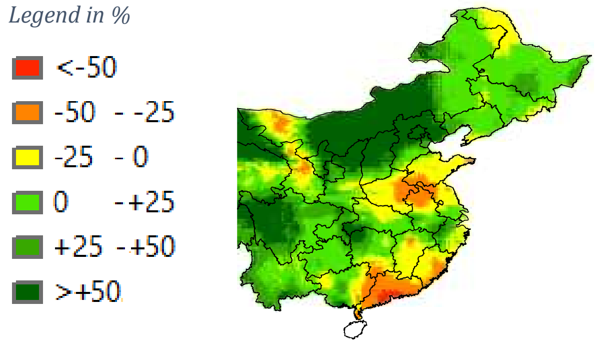

Figure E3. Changes in precipitation in the growing period of maize between 2005 and 2050.

Figure E3 shows the changes in precipitation from 2005 to 2050. It shows that most of the country has an increase in precipitation (green), but the area in the central East, with a lot of planted area will have heavy decreases in precipitation.

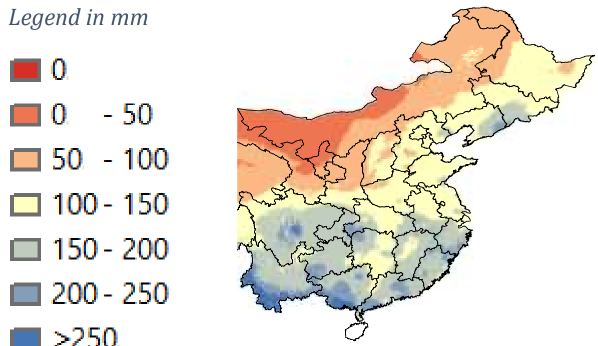

Figure E4. Precipiation in the growing period of maize in 2050.

Figure E4 shows the precipitation over the growing period of maize in 2050. The most significant changes to Figure 2 are that in the central East the monthly precipitation now is only 100-150 mm/month, opposed to 150-200 mm/month in 2005.

Appendix F. Precipitation Changes for Rainfed Wheat under Scenario D85

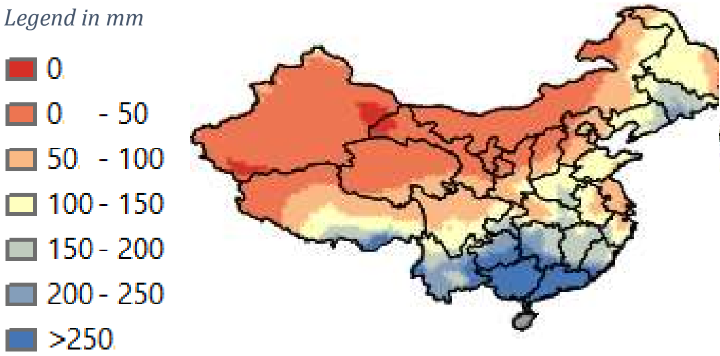

Figure F5. Precipitation in June 2005

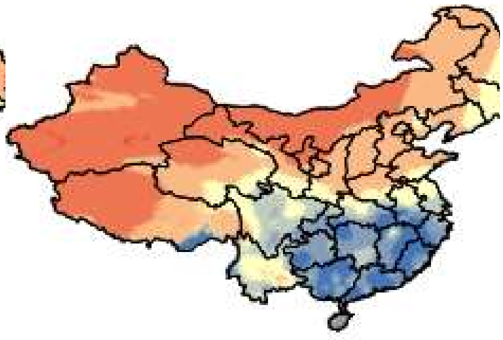

FigureF6. Precipitation in June 2050

Figure F7. June 2005 under 100 mm precipitation area (red), and the 2005 productive RF Wheat area (green)

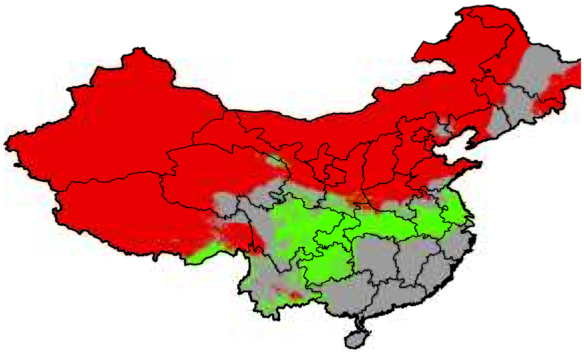

Figure F8. June 2050 under 100 mm precipitation area (red), and the 2050 productive RF wheat area (green)

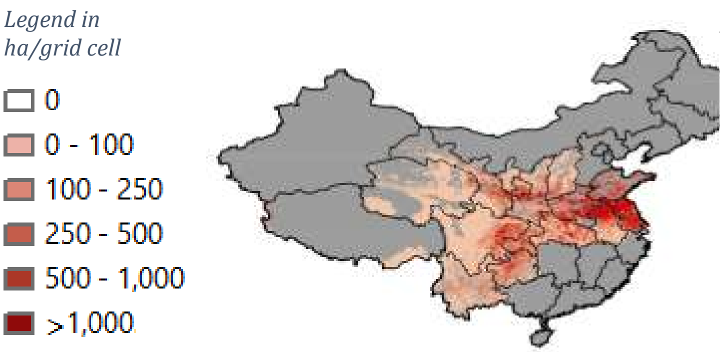

Figure F9. Planted area of RF wheat.

As can be seen in figures F1 and F2, the areas with low precipitation extend further South in 2005 than in 2050. This is better visualised in figures F3 and F4, where the red area has a precipitation lower than 100 mm in the month June. These red areas cover the areas where rainfed wheat fails. This way, the crop fails in Jangsu province and in the north of Anhui province, which is where rainfed wheat has the most ha/grid cell (figure F5), thus causing a major part of the total area to fail.